Impaired Complex-I-Linked Respiration and ATP Synthesis in Primary Open-Angle Glaucoma Patient Lymphoblasts

Shanjean Lee,[1,2] *Leo Sheck,*[3] *Jonathan G. Crowston,*[1] *Nicole J. Van Bergen,*[1] *Evelyn C. O'Neill,*[1] *Fleur O'Hare,*[1] *Yu Xiang George Kong,*[1] *Vicki Chrysostomou,*[1] *Andrea L. Vincent,*[3] *and Ian A. Trounce*[1]

Purpose. Following the recent demonstration of increased mitochondrial DNA mutations in lymphocytes of POAG patients, the authors sought to characterize mitochondrial function in a separate cohort of POAG.

Methods. Using similar methodology to that previous applied to Leber's hereditary optic neuropathy (LHON) patients, maximal adenosine triphosphate (ATP) synthesis and cellular respiration rates, as well as cell growth rates in glucose and galactose media, were assessed in transformed lymphocytes from POAG patients ($n = 15$) and a group of age- and sex-matched controls ($n = 15$).

Results. POAG lymphoblasts had significantly lower rates of complex-I-driven ATP synthesis, with preserved complex-II-driven ATP synthesis. Complex-I driven maximal respiration was also significantly decreased in patient cells. Growth in galactose media, where cells are forced to rely on mitochondrial ATP production, revealed no significant differences between the control and POAG cohort.

Conclusions. POAG lymphoblasts in the study cohort exhibited a defect in complex-I of the oxidative phosphorylation pathway, leading to decreased rates of respiration and ATP production. Studies in LHON and other diseases have established that lymphocyte oxidative phosphorylation measurement is a reliable indicator of systemic dysfunction of this pathway. While these defects did not impact lymphoblast growth when the cells were forced to rely on oxidative ATP supply, the authors suggest that in the presence of a multitude of cellular stressors as seen in the early stages of POAG, these defects may lead to a bioenergetic crisis in retinal ganglion cells and an increased susceptibility to cell death. (*Invest Ophthalmol Vis Sci.* 2012;53:2431–2437) DOI:10.1167/iovs.12-9596

From the [1]Centre for Eye Research Australia, University of Melbourne, Royal Victorian Eye and Ear Hospital, Melbourne, Australia, and the [2]Duke University School of Medicine, Durham, NC, USA, and the [3]Department of Ophthalmology, New Zealand National Eye Centre, Faculty of Medical and Health Sciences, University of Auckland, Auckland, New Zealand.

Supported by the Ophthalmic Research Institute of Australia, Glaucoma Australia Fund, Henry Greenfield Research Fund, Edols Trust Fund, Universitas 21 Doctoral Mobility Scholarship, and the University of Auckland American-Australian Association. The Centre for Eye Research Australia receives operational infrastructure support from the Victorian Government.

Submitted for publication January 30, 2012; revised February 29, 2012; accepted March 2, 2012.

Disclosure: **S. Lee**, None; **L. Sheck**, None; **J.G. Crowston**, None; **N.J. Van Bergen**, None; **E.C. O'Neill**, None; **F. O'Hare**, None; **Y.X.G. Kong**, None; **V. Chrysostomou**, None; **A.L. Vincent**, None; **I.A. Trounce**, None

Corresponding author: Jonathan G. Crowston, Centre for Eye Research Australia, 32 Gisborne Street, East Melbourne, Victoria 3002; crowston@unimelb.edu.au.

Glaucoma is a neurodegenerative disease of the optic nerve characterized by the selective and accelerated loss of retinal ganglion cells (RGCs) and their axons. A growing body of evidence suggests that mitochondrial dysfunction acts causally in a range of neurodegenerative diseases, including Parkinson's disease and Alzheimer's disease.[1] RGCs are specifically sensitive to mitochondrial dysfunction as exemplified by Leber's hereditary optic neuropathy (LHON), mostly caused by a defect in oxidative phosphorylation (OXPHOS) complex-I,[2] and autosomal dominant optic atrophy (ADOA), caused by mutations in nuclear genes encoding a mitochondrial fusion protein *OPA1*.[3,4] Both these diseases share phenotypic similarities, both of which can be mistaken for glaucoma.[5]

Emerging evidence suggests that mitochondrial dysfunction may also contribute to the pathogenesis of glaucomatous optic neuropathy. One genetic analysis has shown a 6- to 8-fold increase in the likelihood of maternal inheritance of POAG,[6] consistent with mitochondrial DNA (mtDNA)-linked risk alleles. Abu-Amero and colleagues[7] found 22 potentially pathogenic mtDNA changes, increases in mtDNA content, and decreased mitochondrial respiratory function in lymphoblasts from a cohort of 27 POAG patients. Somatic mtDNA mutations, which are not inherited, but accumulate with increasing age, may also contribute to mitochondrial dysfunction in glaucoma. The authors have shown that a mouse with neuronal expression of a mutant polymerase gamma gene (*POLG*) has increased mtDNA mutations in the retina and a greater injury response when subjected to acute intraocular pressure (IOP) elevation.[8] An association between polymorphisms in the *OPA1* gene that encodes a mitochondrial structural maintenance protein and increased risk of developing normal tension glaucoma (NTG) and/or POAG has also been observed,[9–12] although some groups have questioned this.[13] These findings provide experimental evidence that mitochondrial dysfunction exists in POAG patients.

In this study, the authors aimed to confirm and further examine the respiratory defects observed by Abu-Amero in a separate cohort of POAG patients by examining maximal rates of cellular adenosine triphosphate (ATP) synthesis, cellular respiration rates, and cell growth rates in lymphoblasts. The utility of using lymphoblast or lymphocyte-derived mitochondria to investigate mitochondrial dysfunction in optic neuropathies has been demonstrated previously in studies that determined OXPHOS defects in LHON[14,15] and ADOA.[16]

Materials and Methods

Patient Recruitment and Demographic Data Collection

Epstein Barr Virus (EBV) transformed lymphoblast lines were obtained from 15 POAG patients, who were recruited through the Glaucoma

Table 1. Patient Demographics

Demographics	Control	POAG
Number of patients	15	15
Age (yrs; mean ± SD)	67.8 ± 9.5	66.7 ± 9.7
Sex	11M, 4F	10M, 5F
Race		
Caucasian	15	11
Asian	0	3
African	0	1

Control and POAG lymphoblasts were matched for age, sex, and race.

Unit at the Royal Victorian Eye and Ear Hospital (East Melbourne, Australia) from November 2008 to August 2009. Inclusion criteria for the study were as follows: evidence of glaucomatous optic neuropathy (loss of the neuroretinal rim and retinal nerve fibre layer loss) with corresponding visual field defect and open angles on gonioscopy. All patients underwent a detailed history and slit-lamp biomicroscopy as well as blood sampling for lymphoblast cell line establishment. The IOP was measured by applanation tonometry (via a Goldmann tonometer) and all assessments were performed at 3 PM ± 1 hour. All patients were receiving treatment for POAG at the time of recruitment. Mean deviation (MD) was used to stratify patients according to severity of disease into 1 of 3 stages: mild >−6 dB; moderate −6 to −12 dB; and severe <−12 dB as previously classified.[17] Tables 1–3 summarize patient history and clinical phenotypes. The tenets of the Declaration of Helsinki were observed, institutional human ethics committee approval was granted, and written informed consent was acquired from all patients.

Cell Lines and Cell Culture Conditions

POAG lymphoblasts were derived from blood samples from 15 POAG patients. Lymphocytes were separated on Ficoll-Paque PLUS gradients (GE Healthcare Biosciences AB, Uppsala, Sweden) and transformed using EBV as previously described.[14] Control cell lines were derived in the same manner and obtained from the HapMap Project of the Coriell Institute of Medical Research (Camden, NJ). The subjects were from the CEPH (Centre d'Etude du Polymorphisme Humain) population (Utah residents with ancestry from northern and western Europe) collected by the International HapMap Project,[18] which has been used as a reference European American population[19] in both functional and genomic studies.[20–22] Control cell lines were age- and sex-matched to the POAG cohort. The authors recently compared mitochondrial function in the HapMap lines with non-mutation carrying control patients in a separate study of ADOA patients and found no discernable difference.[16]

Both POAG and control lymphoblasts were maintained in RPMI-1640 media containing 12 mM glucose, 15% heat-inactivated fetal bovine serum (FBS), 2.05 mM L-glutamine, 100 units/mL penicillin, and 100 μg/mL streptomycin. Lymphoblast lines were also grown in glucose-free galactose RPMI-1640 media, containing 5 mM galactose, 4.5 mM sodium pyruvate, 15% dialyzed heat-inactivated FBS, 2.05 mM L-glutamine, 100 units/mL penicillin, and 100 μg/mL streptomycin. Experiments on galactose-grown lymphoblasts were performed after >9 passages in galactose media. Replacing glucose with galactose as the carbon source forces the cells to produce all ATP by OXPHOS, with no contribution from glycolysis.[23] All lymphoblast lines were cultured as described in 125 cm^2 tissue culture flasks (Greiner Bio-One, Frickenhausen, Germany) and incubated at 37°C, 5% CO_2 in a humidified incubator.

ATP Assay

ATP production rates were determined by using a luciferin/luciferase assay as previously described[24–26] with some modifications. The measurement of mitochondrial ATP synthesis was performed in lymphoblasts grown in RPMI with 12 mM glucose and 15% heat inactivated FBS. Lymphoblasts were re-suspended (7×10^6 cells/mL) in buffer A (10 mM KCl, 25 mM Tris-HCl, 2 mM EDTA, 0.1% bovine serum albumin, 10 mM potassium phosphate, 0.1 mM $MgCl_2$ [pH 7.4]), maintained for 15 minutes at room temperature and subsequently incubated with 50 μg/mL digitonin for 1 minute. After centrifugation, the cell pellet was resuspended in the same volume of buffer A, and aliquots taken to assess ATP synthesis and protein concentration.

Measurements were performed at 30°C in a 96-well luminescent plate reader (FLUOstar Optima, BMG Labtech, Offenburg, Germany) in white-walled, white-based 96-well plates. 50 μL aliquots of digitonin-permeabilized lymphoblasts were incubated for 5 minutes with 50 μL of 25× diluted FLAAM luciferase/luciferin reagent (Sigma, St. Louis, MO) with either 5 mM malate plus 5 mM glutamate (measuring ATP production via complex-I) or with 10 mM succinate plus 2 μg/mL

Table 2. Clinical Characteristics of POAG Cohort

Patient	Family History	Disease Duration (yrs)	Mean Deviation (dB)*	CDR†	IOP (mm Hg)‡	History of Glaucoma Surgery	Number of Medications	History of HTN, DM, HC	Blood Pressure
1	No	13.0	−21.31	0.95	25	Yes	3	HTN	145/75
2	No	18.0	−5.00	0.80	26	No	2	HTN, DM	135/85
3	Yes	6.0	−8.62	0.90	16	No	2	None	110/70
4	Unknown	5.0	−33.65	*0.85*	28	Yes	0	DM	140/80
5	Yes	7.0	−21.70	0.99	37	Yes	0	HC	90/50
6	Yes	29.0	−24.83	0.70	26	Yes	2	None	160/100
7	Yes	4.0	−4.07	0.85	28	No	4	None	170/70
8	Yes	32.0	−4.22	0.90	30	No	2	HTN	130/80
9	Yes	10.0	−31.00	0.99	27	Yes	0	HTN, HC	155/80
10	Yes	2.5	−18.57	0.99	38	Yes	0	HTN, DM, HC	180/100
11	Unknown	3.0	−13.74	0.75	19	No	4	HTN, HC	150/110
12	No	16.0	−21.89	0.95	25	No	4	HTN, DM, HC	145/85
13	No	22.0	−9.70		19	Yes	3	HC	220/110
14	No	3.5	−18.85	0.90	19	No	2	HC	110/70
15	Yes	7.0	−1.99	0.60	27	No	1	HTN, HC	130/70

Yrs, years; CDR, cup-to-disc ratio; HTN, hypertension; DM, diabetes mellitus; HC, hypercholesterolemia.
Mean deviation, CDR, and highest-recorded IOP are reported for more severely affected eye.
* Most recent reliable visual field.
† As assessed on clinical examination and confirmed on optic disc photography.
‡ Highest recorded IOP.

Table 3. Clinical Characteristics of the POAG Cohort

Clinical Characteristics	
Duration of disease (y)	11.9 ± 9.6
Stage of disease	
Mild	4
Moderate	2
Severe	9
Family history	
Yes	8
No	5
Cup-to-disc ratio	0.87 ± 0.12
Intraocular pressure (mm Hg)	26 ± 6.2
History of glaucoma surgery	
Yes	7
No	8
Hypertension	
Yes	9
No	6
Diabetes mellitus	
Yes	3
No	12
Hypercholesterolemia	
Yes	8
No	7
Systolic blood pressure (mm Hg)	142.0 ± 37.6
Diastolic blood pressure (mm Hg)	85.0 ± 14.14

Continuous variables are presented as means, ± standard deviation.

rotenone (measuring ATP production via complex-II). Both complex-I-driven and complex-II-driven reactions were performed in the presence and absence of 10 μg/mL oligomycin, an ATP synthase inhibitor. Luminescence was monitored for 5 minutes prior to the addition of 0.2 mM ADP, after which luminescence was monitored for 30 minutes. The rate of ATP synthesis was linear and dependent on cell density and substrate concentration.

Cellular Respiration

The Oxygraph-2k high-resolution respirometer (Oroboros Instruments, Innsbruck, Austria) was used because the machine can measure slow oxygen consumption rate transitions with superior resolution when compared with conventional oxygen electrodes.[27] All respiration studies were performed at 37°C with a stirrer at 750 rpm. Oxygen consumption was calculated using DatLab software (Oroboros Instruments, Innsbruck, Austria). To standardize instrument performance, the authors performed a daily air calibration on air-saturated media or buffer. Lymphoblast cells (7×10^5 cells/mL) between 48 and 72 hours post passage were re-suspended in respiration buffer (200 mM sucrose, 20 mM taurine, 20 mM HEPES, 10 mM KH_2PO_4, 3 mM $MgCl_2$, 3 mM EGTA, 1 g/L fatty acid free BSA; pH 7.1) as used previously[28] and added to each chamber. Following equilibration for at least 10 minutes with stirring, the chamber was closed. Glutamate (10 mM) and malate (2 mM) were then added, followed by digitonin (10 μg/mL), ADP (1 mM), succinate (10 mM), CCCP (1.5 μM), rotenone (5 μM) and antimycin A (2 μM) at intervals of approximately 2 minutes. Respiration states measured included endogenous respiration rate (with endogenous substrates), ADP stimulated cell respiration with glutamate + malate (CxI-ADP) or with succinate (CxI+II-ADP), and the uncoupled maximal respiration (UC) by the addition of CCCP. On average, the residual oxygen consumption (ROX; when rotenone and antimycin A inhibited mitochondrial respiration) was less than 1% of the UC rate.

Lymphoblast Growth Curves

Lymphoblast viability and number were assessed with the trypan blue exclusion assay. Lymphoblasts were plated in 12 mM glucose or galactose media at an initial cell number of 2.5×10^5 cells. Lymphoblasts were stained with 0.04% (wt/vol) trypan blue and counted using a hemocytometer at 24-hour intervals. Two replicates of the trypan blue exclusion assay were performed per data point. Lymphoblast numbers were also verified using the MTT assay, as described above. Doubling time (DT) was calculated according to the formula: $DT = 0.693t/\ln (N/N_0)$, where t = elapsed time, N_0 = starting number of lymphoblasts, N = final number of lymphoblasts. DT is expressed in hours.

Statistical Analysis

Each experiment was performed with at least 3 replicates, unless otherwise specified. The clinical data are presented as mean values ± standard deviation (SD); experimental data are presented as mean values ± standard error of the mean (SEM). Student's *t*-test and one-way ANOVA were used to assess for statistically significant differences in mitochondrial function between groups. Spearman's rho was calculated using SPSS, Inc. software (IBM, Somner, NY) to assess any correlation between clinical characteristics and mitochondrial function measures. Differences were deemed statistically significant where a P value of $P < 0.05$ was observed.

Results

Patient Demographic Data

Baseline patient demographics are outlined in Table 1 and detailed in Table 2. Mean ages of the control and POAG groups were 67.8 ± 9.5 and 67.3 ± 10.4 years (mean ± SD), respectively. Fifteen control lymphoblast lines from the Coriell Institute of Medical Research from Caucasian donors of northern and western European ancestry were selected to match 15 POAG lymphoblast lines. This control group included 11 males and 4 females; the POAG group included 10 males and 5 females, with a predominantly Caucasian racial makeup (11 of 15 cell lines).

Among the POAG patients, the mean duration of disease was 11.9 ± 9.6 years (mean ± SD; Table 3). All patients had documented visual field defects. Mean deviation (MD) was used to stratify patients according to severity of disease. Based on mean deviation loss, 4 patients had mild, 2 had moderate, and 9 had severe disease. Average cup-to-disc ratio (CDR) was 0.87 ± 0.12, and the mean highest-recorded IOP was 26.0 ± 6.2 mm Hg. Eight patients had a family history of glaucoma, and 7 had undergone glaucoma surgery. Co-morbid conditions included: 3 patients with diabetes, 9 with systemic hypertension, and 8 with hypercholesterolemia. Blood pressures at the time of blood sampling ranged from 110/70 to 220/110, with an average systolic blood pressure (BP) of 142.0 ± 37.6 mm Hg and an average diastolic BP of 85.0 ± 14.1 mm Hg.

POAG Lymphoblasts Have Decreased Rates of Complex-I-Driven ATP Synthesis

To investigate mitochondrial energy production in POAG lymphoblasts, the authors measured the rate of mitochondrial ATP synthesis in digitonin-permeabilized lymphoblasts provided with complex-I substrates (glutamate + malate) or complex-II substrate (succinate + rotenone) in the presence of ADP. Complex-I-driven ATP production rates were significantly lower in POAG lymphoblasts, compared to controls. ATP synthesis rates in the controls were 0.375 ± 0.032 fmoles ATP/sec/10^6 cells and POAG ATP synthesis rates were 0.252 ±

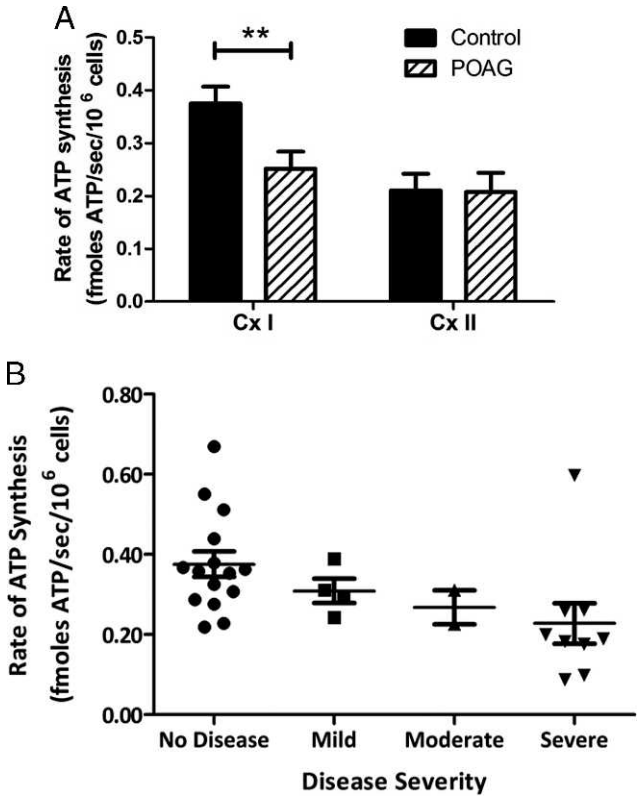

Figure 1. Complex I- and Complex II-driven ATP production in control and POAG lymphoblasts. ATP production rates were assessed in permeabilized control and POAG lymphoblasts. Malate and glutamate were added to drive complex I, and succinate and rotenone were added to drive complex II. (**A**) Decreased rates of complex I-driven ATP production were observed in the POAG lymphoblasts (**$P = 0.01$). (**B**) Reduction in CxI-driven ATP synthesis rates showed a significant correlation with stage of disease as assessed by visual fields ($P = 0.03$), but post-hoc Tukey HSD tests showed no significant differences between mild, moderate, and severe POAG patients.

0.032 fmoles ATP/sec/10^6 cells (33% decrease, $P = 0.001$; Fig. 1). Complex-II-driven rates of ATP synthesis were similar between control and POAG lymphoblasts; ATP production rates were 0.211 ± 0.03 fmoles ATP/sec/10^6 cells in the control group and 0.208 ± 0.03 fmoles ATP/sec/10^6 cells in the POAG group ($P = 0.96$; Fig. 1). In a post-hoc analysis, the authors looked to see if there was an association between complex-I-driven ATP synthesis and stage of glaucoma based on MD value on a 24-2 Humphrey visual field. Figure 1b shows a trend for greater impairment with advancing disease. It is stressed that this study was not designed nor powered to address this substantially, and further work to verify this association is needed.

POAG Lymphoblasts Have Decreased Rates of Complex-I-Driven Cellular Respiration

To further confirm a complex-I defect, the authors measured maximal cellular respiration using a high-resolution oxygraph providing either complex-I or complex-II substrates to the digitonin permeabilized cells in the presence of added ADP. Figure 2 shows that the POAG cells had reduced respiration under all conditions examined, with the difference being statistically significant for endogenous respiration, where controls were 15.4 ± 1.51 pmol/sec/10^6 cells and POAG lymphoblasts were 10.61 ± 1.04 pmol/sec/10^6 cells (30%

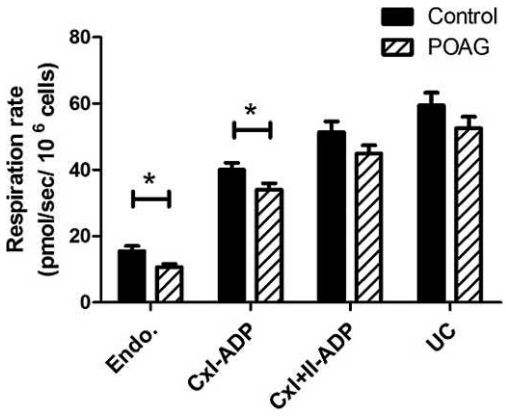

Figure 2. Cellular respiration in control and POAG lymphoblasts. Maximal (ADP-stimulated) respiration of digitonin-permeabilized cells. POAG cells showed a decreased endogenous ($P = 0.016$) and complex-I-linked ($P = 0.047$) respiration. While all other values trended lower in the POAG group, these differences were not statistically significant.

decreased, $P = 0.016$), and complex-I-driven respiration, where controls were 40.05 ± 2.13 and POAGs were 34.04 ± 1.89 pmol/sec/10^6 cells (15% decreased, $P = 0.047$). Although all other values trended lower in the POAG group, these differences were not statistically significant. For complex-I+II-linked respiration, control lymphoblasts were 51.34 ± 3.32 pmol/sec/10^6 cells and POAG lymphoblasts were 44.92 ± 2.53 pmol/sec/10^6 cells ($P = 0.14$), and for maximum uncoupled respiration, controls were 59.41 ± 3.87 and POAGs were 52.54 ± 3.46 pmol/sec/10^6 cells ($P = 0.20$). This suggests that the lower maximal ATP production rates shown in Figure 1 are due at least in part to a lower maximal respiration capacity in POAG lymphoblasts. The lesser impairment in complex-I-driven respiration (15%) compared to complex-I-linked ATP production (33%) could reflect an additional impairment in proton pumping through complex-I in POAG patients, which would lower ATP production in an additive manner.

POAG Control Lymphoblasts Exhibit Similar Growth Rates in Glucose and Galactose Media

Lymphoblast growth curves in standard RPMI-1640 media with 12 mM glucose were similar, with no significant difference between control and POAG lymphoblasts (Fig. 3). Doubling times were 31.2 ± 4.5 hours and 27.0 ± 2.1 hours, respectively. In galactose media, with forced dependence on OXPHOS for energy production, both control and POAG lymphoblasts demonstrated slower growth with corresponding increases in doubling times; 37.7 ± 2.5 hours for control lymphoblasts and 41.0 ± 5.7 for POAG lymphoblasts.

Discussion

Evidence is accumulating that mitochondrial dysfunction may contribute to the underlying pathogenic mechanism of neurodegeneration of the retina and optic nerve in POAG.[7,29,30] Using a well-established lymphoblast-based model to measure systemic mitochondrial function, the authors found that POAG patients had decreased rates of OXPHOS complex-I-driven ATP synthesis, with unchanged complex-II-driven ATP synthesis, suggesting a specific defect in OXPHOS complex I in the study's patient cohort. This was further supported by the authors' finding of a significant defect in maximal complex-I-linked respiration in the same patient cells. Lymphoblast growth rates were unchanged in the POAG cell lines,

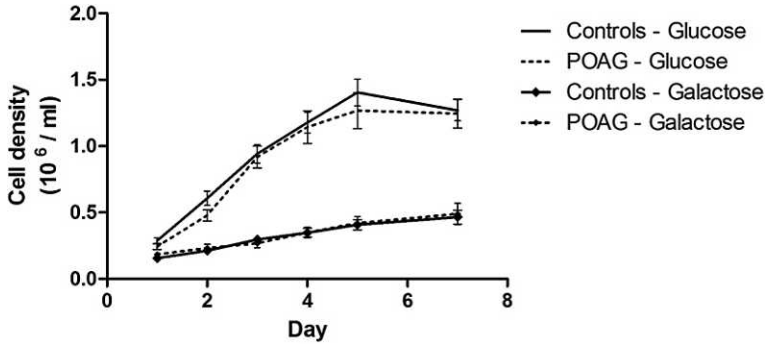

Figure 3. Growth curves for control and POAG patient cells in glucose and galactose. Lymphoblast growth rates were measured in both 12 mM glucose and in glucose-free galactose RPMI media. Both groups of cells grew much more slowly in galactose as expected, while there was no significant difference between the groups at any time point.

suggesting that the complex-I defect does not sufficiently impact lymphoblast growth in-vitro. The ability of lymphoblasts to function normally at baseline coincides with the lack of an obvious widespread systemic phenotype of bioenergetic deficiency in POAG patients.

Increased mitochondrial DNA mutations and non-specific changes in mitochondrial respiration have previously been linked to POAG[7]; however, analysis of OXPHOS has not been performed in POAG. The authors have shown a specific complex-I-linked mitochondrial dysfunction in this POAG cohort. Complex-I (NADH:ubiquinone oxidoreductase) is the largest complex of the electron transport system and is composed of 46 subunits that are encoded by both mtDNA and nuclear genes. Defects in complex-I are the most frequent cause of OXPHOS impairment underlying mitochondrial disease.[31] Defects in complex-I-related OXPHOS function have been associated with a wide spectrum of neurodegenerative diseases, including monosymptomatic optic neuropathies such as LHON and ADOA,[32,33] and are thought to contribute to more phenotypically complicated neurodegenerative diseases including Parkinson's and Alzheimer's disease.[34,35]

The observation of complex-I-linked ATP synthesis defects in POAG lymphoblasts suggests that this defect is also present in cells other than RGCs. The lack of obvious systemic manifestations in POAG patients may be analogous to the tissue-specific manifestation of LHON, in which all cells carry an mtDNA mutation, but only the RGCs demonstrate widespread apoptosis. This might be attributed to the high metabolic requirement in RGCs.[36,37] The RGC axons within the retina are unmyelinated, creating a large demand for ATP in order to propagate action potentials and drive axoplasmic flow.[38–42] The authors speculate that stressors such as increased IOP could place increased bioenergetic demand by restricting axoplasmic flow and potentially lead to bioenergetic crisis in these highly metabolically active neurons. An increased vulnerability to widespread neurodegenerative disease has also been reported; the authors recently described a temporal processing defect in the auditory pathways of glaucoma patients.[43]

The source of decreased complex-I-mediated ATP synthesis in POAG lymphoblasts remains unknown. Mutations in either mtDNA or nuclear DNA may result in complex-I changes that affect electron transfer, proton translocation, or interaction with substrates, all of which may result in less efficient energy production. Abu-Amero and colleagues found 22 potentially pathogenic mtDNA changes spanning the mitochondrial coding region, of which 50% were in complex-I,[7] implying complex-I is a likely candidate for genetic defects in POAG. Although the exact mechanism underlying the selective degeneration of RGCs is unknown, the authors have demonstrated that an increased mtDNA mutation load in the POLG mouse is associated with increased RGC vulnerability to oxidative stress induced by short-term IOP elevation.[8] These findings suggest that OXPHOS impairment limits the optic nerve's ability to withstand injury. There is also evidence that POAG, like LHON and ADOA, is associated with bioenergetic impairment and apoptotic RGC death. Experimentally increased IOP has been shown to result in decreased levels of RGC ATP, both in RGC-5 culture and in animal models.[44,45] Reduced ATP levels have functional consequences manifested as decreased axonal conduction, decreased tolerance for oxygen and glucose deprivation, and increased death of small caliber axons that require high quantities of ATP. Further studies characterizing the nature and origin of the complex-I defect are needed.

The potential limitations to this study include a relatively small sample size, as well as a control and study group derived from different populations; although lymphoblast lines from both groups were established mostly from patients of Caucasian origin, the control lymphoblasts were obtained from a genetic repository of northern European descendants, while the study lymphoblasts were transformed from lymphocytes obtained from a more heterogeneous Caucasian population. If confirmed in larger cohorts of POAG patients, it would be of great interest to examine the potential for mtDNA and nuclear OXPHOS gene polymorphisms contributing to the defects the authors observed. Further work is also required to define the nature of the complex-I defect, and verify whether there is an association with disease stage. Enzymology of OXPHOS complexes requires large sample sizes to detect significant differences, as exemplified by studies in LHON lymphoblast mitochondria, where respiration defects were clearly identified in the absence of complex I enzymatic defects.[14]

In conclusion, the authors present evidence for the presence of a systemic complex-I-linked ATP synthesis defect in POAG patients. This may contribute to the susceptibility of RGCs, which are known to be particularly vulnerable to OXPHOS impairment, to external stressors such as raised IOP. Future studies with larger patient cohorts are required to characterize both the nature and genetic source of the complex-I defect.

References

1. Lin MT, Beal MF. Mitochondrial dysfunction and oxidative stress in neurodegenerative diseases. *Nature*. 2006;443:787–795.
2. Mackey DA, Oostra RJ, Rosenberg T, et al. Primary pathogenic mtDNA mutations in multigeneration pedigrees with Leber

hereditary optic neuropathy. *Am J Hum Genet*. 1996;59:481–485.

3. Alexander C, Votruba M, Pesch UE, et al. OPA1, encoding a dynamin-related GTPase, is mutated in autosomal dominant optic atrophy linked to chromosome 3q28. *Nat Genet*. 2000; 26:211–215.
4. Delettre C, Lenaers G, Griffoin J, et al. Nuclear gene OPA1, encoding a mitochondrial dynamin-related protein, is mutated in dominant optic atrophy. *Nat Genet*. 2000;26:207–210.
5. O'Neill EC, Danesh-Meyer HV, Kong GX, et al. Optic Disc Evaluation in Optic Neuropathies The Optic Disc Assessment Project. *Ophthalmology*. 2011;118(5):964–970.
6. Charliat G, Jolly D, Blanchard F. Genetic risk factor in primary open-angle glaucoma: a case-control study. *Ophthalmic Epidemiol*. 1994;1:131–138.
7. Abu-Amero KK, Morales J, Bosley TM. Mitochondrial abnormalities in patients with primary open-angle glaucoma. *Invest Ophthalmol Vis Sci*. 2006;47:2533–2541.
8. Kong YX, Van Bergen N, Trounce IA, et al. Increase in mitochondrial DNA mutations impairs retinal function and renders the retina vulnerable to injury. *Aging Cell*. 2011;10(4): 572–583.
9. Aung T, Ocaka L, Ebenezer ND, et al. Investigating the association between OPA1 polymorphisms and glaucoma: comparison between normal tension and high tension primary open angle glaucoma. *Hum Genet*. 2002;110:513–514.
10. Aung T, Ocaka L, Ebenezer ND, et al. A major marker for normal tension glaucoma: association with polymorphisms in the OPA1 gene. *Hum Genet*. 2002;110:52–56.
11. Mabuchi F, Tang S, Kashiwagi K, Yamagata Z, Iijima H, Tsukahara S. The OPA1 gene polymorphism is associated with normal tension and high tension glaucoma. *Am J Ophthalmol*. 2007;143:125–130.
12. Powell BL, Toomes C, Scott S, et al. Polymorphisms in OPA1 are associated with normal tension glaucoma. *Mol Vis*. 2003;9: 460–464.
13. Yu-Wai-Man P, Stewart JD, Hudson G, et al. OPA1 increases the risk of normal but not high tension glaucoma. *J Med Genet*. 2010;47(2):120–125.
14. Brown MD, Trounce IA, Jun AS, Allen JC, Wallace DC. Functional analysis of lymphoblast and cybrid mitochondria containing the 3460, 11778, or 14484 Leber's hereditary optic neuropathy mitochondrial DNA mutation. *J Biol Chem*. 2000; 275:39831–39836.
15. Brown MD, Allen JC, Van Stavern GP, Newman NJ, Wallace DC. Clinical, genetic, and biochemical characterization of a Leber hereditary optic neuropathy family containing both the 11778 and 14484 primary mutations. *Am J Med Genet*. 2001;104: 331–338.
16. Van Bergen N, Crowston J, Kearns L, et al. Mitochondrial oxidative phosphorylation compensation may preserve vision in patients with OPA1-linked autosomal dominant optic atrophy. *PLoS One*. 2011;6:e21347.
17. Hodapp E, Parrish RK, Anderson DR. Clinical Decisions in Glaucoma. St Louis: The CV Mosby Co; 1993:52–61.
18. Gibbs RA, Belmont JW, Hardenbol P, et al. The International HapMap Project. *Nature*. 2003;426:789–796.
19. Meucci MA, Marsh S, Watters JW, McLeod HL. CEPH individuals are representative of the European American population: implications for pharmacogenetics. *Pharmacogenomics*. 2005;6:59–63.
20. Garcia-Barcelo M, So MT, Lau DK, et al. Population differences in the polyalanine domain and 6 new mutations in HLXB9 in patients with Currarino syndrome. *Clin Chem*. 2006;52:46–52.
21. Pottier N, Cheok MH, Yang W, et al. Expression of SMARCB1 modulates steroid sensitivity in human lymphoblastoid cells: identification of a promoter SNP that alters PARP1 binding and SMARCB1 expression. *Hum Mol Genet*. 2007;16:2261–2271.
22. Trevino LR, Yang W, French D, et al. Germline genomic variants associated with childhood acute lymphoblastic leukemia. *Nat Genet*. 2009;41:1001–1005.
23. Robinson BH, Petrova-Benedict R, Buncic JR, Wallace DC. Nonviability of cells with oxidative defects in galactose medium: a screening test for affected patient fibroblasts. *Biochem Med Metab Biol*. 1992;48:122–126.
24. Bonora E, Porcelli AM, Gasparre G, et al. Defective oxidative phosphorylation in thyroid oncocytic carcinoma is associated with pathogenic mitochondrial DNA mutations affecting complexes I and III. *Cancer Res*. 2006;66:6087–6096.
25. Zanna C, Ghelli A, Porcelli AM, Martinuzzi A, Carelli V, Rugolo M. Caspase-independent death of Leber's hereditary optic neuropathy cybrids is driven by energetic failure and mediated by AIF and Endonuclease G. *Apoptosis*. 2005;10:997–1007.
26. Manfredi G, Yang L, Gajewski CD, Mattiazzi M. Measurements of ATP in mammalian cells. *Methods*. 2002;26:317–326.
27. Hutter E, Unterluggauer H, Garedew A, Jansen-Durr P, Gnaiger E. High-resolution respirometry–a modern tool in aging research. *Exp Gerontol*. 2006;41:103–109.
28. Stadlmann S, Rieger G, Amberger A, Kuznetsov AV, Margreiter R, Gnaiger E. H2O2-mediated oxidative stress versus cold ischemia-reperfusion: mitochondrial respiratory defects in cultured human endothelial cells. *Transplantation*. 2002;74: 1800–1803.
29. Carelli V, Ross-Cisneros FN, Sadun AA. Mitochondrial dysfunction as a cause of optic neuropathies. *Prog Retin Eye Res*. 2004;23:53–89.
30. Kong GY, Van Bergen NJ, Trounce IA, Crowston JG. Mitochondrial dysfunction and glaucoma. *J Glaucoma*. 2009;18:93–100.
31. Smeitink J, van den Heuvel L, DiMauro S. The genetics and pathology of oxidative phosphorylation. *Nat Rev Genet*. 2001; 2:342–352.
32. Chevrollier A, Guillet V, Loiseau D, et al. Hereditary optic neuropathies share a common mitochondrial coupling defect. *Ann Neurol*. 2008;63:794–798.
33. Carelli V, La Morgia C, Iommarini L, et al. Mitochondrial optic neuropathies: how two genomes may kill the same cell type? *Biosci Rep*. 2007;27:173–184.
34. Kwong JQ, Beal MF, Manfredi G. The role of mitochondria in inherited neurodegenerative diseases. *J Neurochem*. 2006;97: 1659–1675.
35. Schapira AH. Complex I: inhibitors, inhibition and neurodegeneration. *Experimental neurology*. 2010;224:331–335.
36. Raichle ME, Gusnard DA. Appraising the brain's energy budget. *Proc Natl Acad Sci U S A*. 2002;99:10237–10239.
37. Yu DY, Cringle SJ. Oxygen distribution and consumption within the retina in vascularised and avascular retinas and in animal models of retinal disease. *Prog Retin Eye Res*. 2001;20: 175–208.
38. Andrews RM, Griffiths PG, Johnson MA, Turnbull DM. Histochemical localisation of mitochondrial enzyme activity in human optic nerve and retina. *Br J Ophthalmol*. 1999;83: 231–235.
39. Bristow EA, Griffiths PG, Andrews RM, Johnson MA, Turnbull DM. The distribution of mitochondrial activity in relation to optic nerve structure. *Arch Ophthalmol*. 2002;120:791–796.
40. Hollander H, Makarov F, Stefani FH, Stone J. Evidence of constriction of optic nerve axons at the lamina cribrosa in the normotensive eye in humans and other mammals. *Ophthalmic Res*. 1995;27:296–309.
41. Minckler DS, Bunt AH, Johanson GW. Orthograde and retrograde axoplasmic transport during acute ocular hyper-

tension in the monkey. *Invest Ophthalmol Vis Sci*. 1977;16: 426–441.

42. Mutsaers SE, Carroll WM. Focal accumulation of intra-axonal mitochondria in demyelination of the cat optic nerve. *Acta Neuropathol*. 1998;96:139–143.
43. Rance G, O'Hare F, O'Leary S, et al. Auditory processing deficits in individuals with primary open-angle glaucoma. *Int J Audiol*. 2012;51:10–15.
44. Ju WK, Liu Q, Kim KY, et al. Elevated hydrostatic pressure triggers mitochondrial fission and decreases cellular ATP in differentiated RGC-5 cells. *Invest Ophthalmol Vis Sci*. 2007; 48:2145–2151.
45. Baltan S, Inman DM, Danilov CA, Morrison RS, Calkins DJ, Horner PJ. Metabolic vulnerability disposes retinal ganglion cell axons to dysfunction in a model of glaucomatous degeneration. *J Neurosci*. 2010;30:5644–5652.